THE UNIVERSITY of EDINBURGH

Edinburgh Research Explorer

Performance Analysis of IA Techniques in the MIMO IBC With Imperfect CSI

OPEN ACCESS

Performance Analysis of IA Techniques in the MIMO IBC With Imperfect CSI

Paula Aquilina, *Student Member, IEEE*, and Tharmalingam Ratnarajah, *Senior Member, IEEE*

Abstract—In this work we consider the multiple-input multiple-output (MIMO) interference broadcast channel (IBC) and analyse the performance of interference alignment (IA) under imperfect channel state information (CSI), where the variance of the CSI error depends on the signal-to-noise ratio (SNR). First, we derive an upper bound on asymptotic mean loss in sum rate compared to the perfect CSI case and then we quantify the achievable degrees of freedom (DoF) with imperfect CSI. Both sum rate loss and achievable DoF are found to be dependent on the number of cells in the system and the amount of users per cell, in addition to the CSI error parameters themselves. Results show that when error variance is inversely proportional to SNR, full DoF are achievable and the asymptotic sum rate loss is bounded by a derived value. Additionally if the CSI imperfection does not disappear for asymptotically high SNR, then the full DoF gain promised by IA cannot be achieved; we quantify this loss in relation to the CSI mismatch itself. The analytically derived bounds are validated via system simulation, with the cellular counterparts of the maximum signal-to-interference-plus-noise ratio (Max-SINR) and the minimum weighted leakage interference (Min-WLI) algorithms being the IA techniques of choice. Secondly, inspired by the CSI mismatch model used to derive the bounds, we present a novel Max-SINR algorithm with stochastic CSI error knowledge (Max-SINR-SCEK) for the MIMO IBC. Simulations show that the proposed algorithm improves performance over the standard one under imperfect CSI conditions, without any additional computational costs.

Index Terms—Degrees of freedom, imperfect CSI, interference alignment, MIMO interference broadcast channel.

I. Introduction

SPECTRAL efficiency is a key performance metric when it comes to the design of cellular systems. However, the users' throughput capability is greatly limited by interference from other co-channel users within the same cell or from neighbouring ones. Thus finding ways to handle this interference effectively is fundamental. Interference alignment (IA) is a relatively recent solution to the problem [1]. It aims to align

unwanted signals into a restricted subspace that is smaller than the number of interferers themselves. Additionally it has been shown that via the use of IA the achievable degrees of freedom (DoF) scale up linearly with the number of users for the interference channel (IC) [2], rendering it a highly promising technique in theory.

Nonetheless there are a number of issues which impact the applicability of IA in a realistic setting [3]. One of the most common prerequisites for the implementation of IA solutions is the instantaneous availability of perfect channel state information (CSI) at both the transmitter and the receiver to achieve full DoF. This perfect CSI assumption is highly idealistic; in practice the available CSI is usually an imperfect estimate which causes performance loss both in terms of sum rate and achievable DoF. Thus it is important to fully understand to what extent imperfect CSI knowledge degrades IA performance. A substantial amount of work in literature focuses on imperfection due to quantisation. For example it has been shown that for IA techniques with quantised CSI feedback, optimal DoF can still be achieved as long as the feedback bit rate scales sufficiently fast with signal-to-noise ratio (SNR) for both single-input single-output (SISO) [4] and multiple-input multiple-output (MIMO) ICs [5]. Aside from imperfection due to quantisation, performance analysis of IA under generalised CSI mismatch is of great interest, however due to the complex nature of the issue different works deal with various CSI uncertainty aspects separately. For example the DoF achievable by IA over correlated channels with imperfect CSI has been investigated in [6], while [7] deals with the performance analysis of IA in systems with analog channel state feedback. Also, [8] derives upper and lower bounds on the sum mutual information where the variance of the CSI error is considered as a constant.

Most of the works mentioned so far deal with multiple point-to-point interfering links, however IA can also be used to increase throughput within the context of cellular systems with more than one user per cell. For example, [9] develops an uplink scheme that approaches interference-free DoF as the number of users in each cell increases. Other works directly investigate the achievable DoF for the MIMO interference broadcast channel (IBC), initially for simple two-cell systems [10], [11] and more recently for cellular systems with a varying number of cells [13]–[16].

When it comes to IA and its usability, it is not sufficient to solely characterise the achievable DoF; we also require knowledge of the minimum number of transmit and receive antennas that guarantee IA feasibility. Such analysis for the MIMO IBC is complex due to the nature of the channel itself. For example [17] and [18] provide feasibility conditions for

linear IA in various subclasses of the fully-connected MIMO IBC, while [19] deals with partially-connected systems.

This work focuses on the performance analysis of IA techniques in the presence of imperfect CSI in a MIMO IBC setup. The CSI mismatch model used is versatile and allows us to treat error variance either as a function of SNR or as independent of it. Thus for example, just by changing the error parameter specifications it can be used to represent both reciprocal channels and channels which acquire CSI at the transmitter via quantised feedback. A similar model has been applied to the MIMO IC in [20] and also to vector perturbation precoding in [21]. Given this error model, in the first part of our work we derive bounds on the sum rate loss and the achievable DoF for the MIMO IBC. Results show that when the error variance is inversely proportional to SNR, full DoF can be achieved, moreover the asymptotic sum rate loss is shown to be bounded by a derived value dependent on the system parameters and the CSI imperfection. Additionally in cases where the CSI imperfection does not disappear with asymptotically high SNR, full DoF cannot be obtained. This occurs when error variance depends on SNR to the power of a proper fraction; we quantify this DoF loss and also show that for the same scenario the asymptotic sum rate loss is unbounded.

In the second part of this work we consider various IA schemes that can be applied to the MIMO IBC. We start by outlining two standard IA techniques that are later used to verify the validity of the derived bounds. The chosen methods are the maximum signal-to-interference-plus-noise ratio (Max-SINR) and the minimum weighted leakage interference (Min-WLI) algorithms. Both were initially proposed for the MIMO IC in [22] and are widely used as benchmark algorithms. A straightforward extension to the MIMO IBC does not provide optimal results [23]–[25]. Thus, here we present and apply their cellular multi-stream counterparts.

Next, we place our focus on the performance of the Max-SINR algorithm under CSI mismatch. This technique is interesting because rather than minimizing the leaked interference directly, it aims to maximise the signal-to-interference-plus-noise ratio on a stream-by-stream basis. It is given high relevance in literature since it has been found to outperform other techniques. For example, [26] establishes its optimality within the class of linear beamforming algorithms at high SNR and [27] shows that it achieves better throughput than sum rate gradient algorithms at low-to-intermediate SNRs. Its convergence behaviour has also been analysed in [28]. However, most prior works are for the IC in a perfect CSI scenario. Therefore inspired by the imperfect CSI model used to derive the bounds, we propose a novel version of the Max-SINR algorithm for the IBC. Our algorithm exploits stochastic knowledge on the CSI mismatch to counter its negative impact. Results show that the proposed method does indeed provide performance improvements when compared to the standard version and at no extra computational cost.

The rest of this paper is organised as follows. Section II specifies the MIMO IBC system and the CSI mismatch model used, while Section III gives an overview of the performance of IA under perfect CSI. In Section IV we deal with the performance analysis of IA under imperfect CSI conditions,

presenting two theorems that separately define the asymptotic sum rate loss and quantify the achievable DoF. Next, Section V gives an overview of IA schemes for the MIMO IBC; the first part focuses on standard schemes used to verify the derived theorems, while the second part introduces a novel version of the Max-SINR algorithm which exploits stochastic knowledge on the CSI uncertainty. In Section VI we provide simulation results confirming the validity of the presented theorems and the performance benefits of the novel Max-SINR algorithm. Finally, Section VII provides some concluding remarks. Additionally, there are also three appendices, the first one outlines some useful lemmas, while the last two offer proofs of the analytical results.

Notation: We use lower case standard font for scalars, lower case bold font for vectors and upper case bold font for matrices. $|\cdot|$ denotes the absolute value, while $\|\cdot\|$ indicates the Euclidean 2-norm. $\text{Tr}(\mathbf{A})$ represents the trace of matrix $\mathbf{A}$. $\mathbf{A}^{\dagger}$ indicates the pseudo-inverse of $\mathbf{A}$. Also, $\mathcal{V}_n[\mathbf{A}]$ is defined as the set of eigenvectors corresponding to the n smallest eigenvalues of $\mathbf{A}$.

II. SYSTEM MODEL

We consider a symmetric G-cell MIMO IBC network, where every cell has K users, each equipped with N antennas. There is one base-station (BS) having M antennas per cell. For this system, D is defined as the number of streams intended for each user separately and it is assumed that the choice of system parameters is such that IA is feasible.

The received signal for user k in cell g is given by

$$\widehat{\mathbf{x}}_{k_g} = \underbrace{\mathbf{U}_{k_g}^H \mathbf{H}_{k_g,g} \mathbf{V}_{k_g} \mathbf{x}_{k_g}}_{\text{desired signal}} + \underbrace{\sum_{\substack{l=1 \\ l \neq k}}^{K} \mathbf{U}_{k_g}^H \mathbf{H}_{k_g,g} \mathbf{V}_{l_g} \mathbf{x}_{l_g}}_{\text{intra-cell interference}}$$

$$+ \underbrace{\sum_{\substack{j=1 \\ j \neq g}}^{G} \sum_{l=1}^{K} \mathbf{U}_{k_g}^H \mathbf{H}_{k_g,j} \mathbf{V}_{l_j} \mathbf{x}_{l_j}}_{\text{inter-cell interference}} + \underbrace{\mathbf{U}_{k_g}^H \mathbf{w}_{k_g}}_{\text{noise}} \quad (1)$$

where $\mathbf{x}_{l_j} \in \mathbb{C}^{D \times 1}$ is the transmitted symbol vector for user l in cell j, satisfying $\mathbb{E}\{\mathbf{x}_{l_j}^H \mathbf{x}_{l_j}\} \leq PD$; $\mathbf{V}_{l_j} \in \mathbb{C}^{M \times D}$ is the unit-norm transmit beamforming matrix for user l_j satisfying $\text{Tr}(\mathbf{V}_{l_j} \mathbf{V}_{l_j}^H) = D$; $\mathbf{U}_{k_g} \in \mathbb{C}^{N \times D}$ is the receive beamforming matrix for user k_g; $\mathbf{H}_{k_g,j} \in \mathbb{C}^{N \times M}$ is the channel link from BS j to user k_g, with each element being drawn from a normal distribution with zero mean and variance one, and finally $\mathbf{w}_{k_g} \in \mathbb{C}^{N \times 1}$ represents additive white Gaussian noise (AWGN) with variance σ^2. A simple MIMO IBC with $G = 2$ is shown in Fig. 1.

For the system specified in (1) the following conditions need to be satisfied to achieve IA

$$\text{rank}\left(\mathbf{U}_{k_g}^H \mathbf{H}_{k_g,g} \mathbf{V}_{k_g}\right) = D, \quad \forall k, g$$

$$\mathbf{U}_{k_g}^H \mathbf{H}_{k_g,g} \mathbf{V}_{l_g} = 0, \quad \forall l \neq k$$

$$\mathbf{U}_{k_g}^H \mathbf{H}_{k_g,j} \mathbf{V}_{l_j} = 0, \quad \forall j \neq g. \quad (2)$$
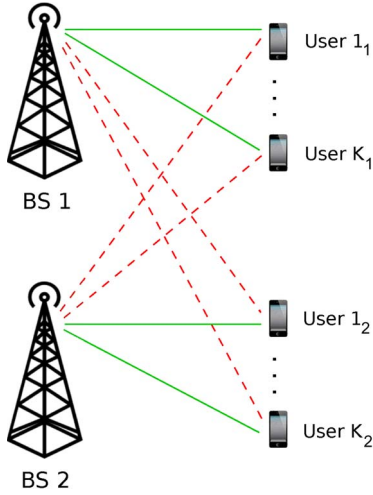
Fig. 1. Two-cell MIMO IBC with green solid lines representing direct links and red dashed lines representing inter-cell links.

In this work we are concerned with the effect of imperfect CSI on IA performance, thus we define the following model for the CSI mismatch

$$\widehat{\mathbf{H}} = \mathbf{H} + \mathbf{E} \tag{3}$$

where $\widehat{\mathbf{H}}$ represents the observed mismatched CSI, $\mathbf{H} \sim \mathcal{CN}(0, \mathbf{I})$ is the actual channel matrix and $\mathbf{E}$ is the error matrix representing the degree of inaccuracy in the observed CSI. The error matrix $\mathbf{E}$ is assumed to be independent of $\mathbf{H}$. Defining the nominal SNR as $\rho \triangleq \frac{P}{\sigma^2}$, then $\mathbf{E}$ is modelled as

$$\mathbf{E} \sim \mathcal{CN}(0, \eta \mathbf{I}) \text{ with } \eta \triangleq \beta \rho^{-\alpha}. \tag{4}$$

With this model the error variance, η, can be used to capture a variety of CSI acquisition scenarios for any constants $\alpha \geq 0$ and $\beta > 0$. Of particular interest are the instances highlighted next.

1) Perfect CSI: As $\alpha \to \infty$ perfect CSI is obtained, for $\rho > 1$.

2) Reciprocal Channels: For reciprocal systems (e.g. time-division duplex) users transmit pilots over the uplink, based on which channel information is obtained at the BS. This CSI knowledge is applicable for both uplink and downlink channels, due to reciprocity. Therefore in this case CSI error is dependent on the ratio of pilot power to noise level at the BS, i.e. it is inversely proportional to SNR, which can be modelled by setting $\alpha = 1$ in (4).

3) CSI Feedback: In non-reciprocal systems (e.g. frequency-division duplex) uplink and downlink are considered to be independent. Pilots are transmitted by the BS to the users, allowing the receivers to obtain the downlink information. Given the lack of reciprocity, this information can only be supplied to the BS via a dedicated feedback link. Data sent over this link is quantised, thus the major contributor to the CSI mismatch is the quantisation process itself. The resulting error is independent of SNR, thereby the scenario can be modelled by setting $\alpha = 0$ in (4).

Alternatively the error variance, η, as a whole can be interpreted as a single parameter that encapsulates the quality of the CSI. Its value may be assumed to be known *a priori* and

can be determined depending on the channel dynamics and the channel estimation schemes applied (see for example [29] and references within).

For our performance analysis we require the statistical properties of the actual channel $\mathbf{H}$ conditioned on $\widehat{\mathbf{H}}$. Since $\widehat{\mathbf{H}} = \mathbf{H} + \mathbf{E}$, with $\mathbf{H}$ and $\mathbf{E}$ being statistically independent Gaussian variables, then $\widehat{\mathbf{H}}$ and $\mathbf{H}$ are jointly Gaussian. Therefore conditioned on $\widehat{\mathbf{H}}$, $\mathbf{H}$ is Gaussian distributed with mean $\widehat{\mathbf{H}}/(1 + \eta)$ and statistically independent elements of variance $\eta/(1 + \eta)$ [30]. Thus the actual channel can be expressed as

$$\mathbf{H} = \frac{1}{1 + \eta} \widehat{\mathbf{H}} + \mathbf{\Upsilon} \tag{5}$$

where $\mathbf{\Upsilon}$ is independent of $\widehat{\mathbf{H}}$, with distribution

$$\mathbf{\Upsilon} \sim \mathcal{CN}\left(0, \frac{\eta}{1 + \eta} \mathbf{I}\right). \tag{6}$$

III. ACHIEVABLE DoF AND SUM RATE WITH PERFECT CSI

Our analysis is concerned with the performance degradation in systems where the available CSI is imperfect. Since we focus on the sum rate and DoF loss, it is useful to first define the performance achieved with perfect CSI for comparison purposes. Assuming diagonalised sub-channels, the IA conditions in (2) can be expressed on a per-stream basis as

$$\left|\mathbf{u}_{k_g}^{dH} \mathbf{H}_{k_g, g} \mathbf{v}_{k_g}^{d}\right| > 0, \ \forall d, k, g$$
$$\mathbf{u}_{k_g}^{dH} \mathbf{H}_{k_g, j} \mathbf{v}_{l_j}^{m} = 0, \ \forall (d, k, g) \neq (m, l, j) \tag{7}$$

where $\mathbf{u}_{k_g}^{d}$ refers to the dth column of $\mathbf{U}_{k_g}$ and $\mathbf{v}_{l_j}^{m}$ refers to the mth column of $\mathbf{V}_{l_j}$.

Considering i.i.d. Gaussian inputs and the fact there is no interference leakage with perfect CSI, then the achievable sum rate is given by

$$R_{\text{perfect CSI}} = \sum_{g=1}^{G} \sum_{k=1}^{K} \sum_{d=1}^{D} \log_2 \left(1 + \frac{P \left|\mathbf{u}_{k_g}^{dH} \mathbf{H}_{k_g, g} \mathbf{v}_{k_g}^{d}\right|^2}{\sigma^2}\right). \tag{8}$$

We are also interested in the DoF analysis. This property is related to sum rate as

$$DoF = \lim_{P \to \infty} \frac{R}{\log_2 P}. \tag{9}$$

Provided that the IA feasibility conditions are met, we can use the sum rate to DoF relationship in (9) to calculate the DoF achievable with perfect CSI as

$$DoF_{\text{perfect CSI}} = \lim_{P \to \infty} \frac{R_{\text{perfect CSI}}}{\log_2 P} = GKD \tag{10}$$

where $R_{\text{perfect CSI}}$ is defined in (8). The last equality follows by taking expectations, using the easily shown fact that $|\mathbf{u}_{k_g}^{d\,H} \mathbf{H}_{k_g, g} \mathbf{v}_{k_g}^{d}|^2$ is exponentially distributed with zero mean and variance one, and finally taking the limit $P \to \infty$.

IV. PERFORMANCE ANALYSIS UNDER IMPERFECT CSI

When it comes to the imperfect CSI scenario, the information available for the calculation of precoders and combiners is only an imperfect observation of the actual channel state; thus all beamformers are calculated using $\widehat{\mathbf{H}}$ rather than $\mathbf{H}$. This implies that instead of the original IA conditions in (7), the alignment conditions observed are

$$\left|\widehat{\mathbf{u}}_{k_g}^{dH}\widehat{\mathbf{H}}_{k_g,g}\widehat{\mathbf{v}}_{k_g}^d\right| > 0, \ \forall \, d, k, g$$

$$\widehat{\mathbf{u}}_{k_g}^{dH}\widehat{\mathbf{H}}_{k_g,j}\widehat{\mathbf{v}}_{l_j}^m = 0, \ \forall \, (d, k, g) \neq (m, l, j) \quad (11)$$

where the beamformers $\widehat{\mathbf{u}}$ and $\widehat{\mathbf{v}}$ are calculated using the mismatched channel information, $\widehat{\mathbf{H}}$. Satisfying the modified IA conditions in (11) leads to some residual leakage interference, equivalent to (12) below.

$$\widehat{J}_{k_g}^d = \sum_{\substack{m=1 \\ m \neq d}}^{D} P \left|\widehat{\mathbf{u}}_{k_g}^{dH}\mathbf{H}_{k_g,g}\widehat{\mathbf{v}}_{k_g}^m\right|^2 + \sum_{\substack{l=1 \\ l \neq k}}^{K} \sum_{m=1}^{D} P \left|\widehat{\mathbf{u}}_{k_g}^{dH}\mathbf{H}_{k_g,g}\widehat{\mathbf{v}}_{l_g}^m\right|^2$$

$$+ \sum_{\substack{j=1 \\ j \neq g}}^{G} \sum_{l=1}^{K} \sum_{m=1}^{D} P \left|\widehat{\mathbf{u}}_{k_g}^{dH}\mathbf{H}_{k_g,j}\widehat{\mathbf{v}}_{l_j}^m\right|^2 \quad (12)$$

Residual leakage has a negative impact on the sum rate and DoF achievable by the system. Understanding the extent of this loss is fundamental, because it gives a more realistic characterisation of system performance. Here we present two theorems that separately quantify the asymptotic sum rate loss and the decrease in achievable DoF.

A. Sum Rate Loss With Imperfect CSI

Sum rate loss, ΔR, is defined as the difference between the sum rate achievable with perfect CSI from (8) and the sum rate achievable with imperfect CSI given by

$$R_{\text{imperfect CSI}} = \sum_{g=1}^{G} \sum_{k=1}^{K} \sum_{d=1}^{D} \log_2 \left(1 + \frac{P \left|\widehat{\mathbf{u}}_{k_g}^{dH}\mathbf{H}_{k_g,g}\widehat{\mathbf{v}}_{k_g}^d\right|^2}{\widehat{J}_{k_g}^d + \sigma^2}\right). \quad (13)$$

Given this definition, we can now refer to the following theorem.

Theorem 1: For the symmetric MIMO IBC under imperfect CSI with error variance, $\eta = \beta\rho^{-\alpha}$, at asymptotically high SNR: ΔR tends to zero for $\alpha > 1$, tends to infinity for $0 \leq \alpha < 1$ and for $\alpha = 1$ is finite and upper bounded by $GKD \log_2(1 + \beta(GKD - 1))$, i.e.

$$\lim_{SNR \to \infty} \Delta R \begin{cases} = 0 & \alpha > 1 \\ \leq GKD \log_2(1 + \beta(GKD - 1)) & \alpha = 1 \\ = \infty & 0 \leq \alpha < 1. \end{cases} \quad (14)$$

Proof: The proof is given in Appendix B. ∎

B. DoF Loss With Imperfect CSI

The DoF loss, ΔDoF, is defined as the difference between the DoF achievable with perfect CSI and the DoF achievable

under imperfect CSI. Given this definition, we can now refer to the following theorem.

Theorem 2: For the symmetric MIMO IBC under imperfect CSI with error variance, $\eta = \beta\rho^{-\alpha}$, full DoF can be achieved for values of $\alpha \geq 1$, while in the range of $0 \leq \alpha < 1$ the DoF loss is equivalent to a fraction of $(1 - \alpha)$ of the full DoF, which can be summarised as

$$\Delta DoF = \begin{cases} 0 & \alpha \geq 1 \\ (1 - \alpha)DoF_{\text{perfect CSI}} & 0 \leq \alpha < 1. \end{cases} \quad (15)$$

Proof: The proof is given in Appendix C. ∎

Remark 1: Note that the implications of the two theorems presented in this section are intrinsically related. For example, in the range of $\alpha \geq 1$ Theorem 1 indicates the sum rate loss is either zero or finite, which is directly reflected in Theorem 2 where no DoF loss is expected within the same α range. On the other hand for the case where $0 \leq \alpha < 1$, Theorem 2 indicates that a DoF loss is inevitable. This is also reflected in Theorem 1, which states that the sum rate loss increases unboundedly with SNR for the same range of α values.

V. IA SCHEMES FOR THE MIMO IBC

To test the bounds presented in Section IV we require the use of IA schemes for the MIMO IBC. Here we apply adapted versions of the Max-SINR and Min-WLI algorithms originally proposed for the IC in [22]. While the first part of this section provides an outline of these two schemes; in the second subsection we focus solely on the Max-SINR algorithm and present a novel version that exploits stochastic knowledge of the CSI uncertainty to improve performance. We refer to this algorithm as Max-SINR with stochastic CSI error knowledge (Max-SINR-SCEK).

A. Standard IA Schemes Adapted to the MIMO IBC

Since the original Max-SINR and Min-WLI algorithms from [22] were developed for the IC, they are unable to cater for intra-cell interference. When it comes to adapting them to the IBC, various works in literature propose different ways on how to handle this additional interference component. Thus in this subsection we outline an adapted version of each, which we later use to obtain the simulation results in Section VI-A.

1) Max-SINR for the MIMO IBC: This algorithm focuses on maximising the signal-to-interference-plus-noise ratio on a per stream basis, to create a desired signal subspace that contains the required number of interference free dimensions. A direct extension from [22] would involve calculating both the transmit and receive filters based on the total interference plus noise covariance matrix, which for the MIMO IBC also includes intra-cell interference. Our simulations of the direct extension have shown that is not always able to achieve the desired alignment results over the whole SNR range. For tightly feasible cases, as SNR increases the sum rate saturates due to convergence issues. This under performance has also been reported in [23] and [24] for single-stream cellular systems.

Solutions proposed separately in [23] and [24] avoid this behaviour by ignoring intra-cell interference in the transmit

subspace. The adapted Max-SINR algorithm outlined in Algorithm 1 applies a similar principle, while still retaining an underlying multi-stream structure that mirrors the original algorithm from [22]. Thus the receive filters are concerned only with inter-cell interference, while the transmit filters deal with both inter-cell and intra-cell interference when calculating the forward and backward interference plus noise covariance matrices, given by $\mathbf{Q}_{k_g}^d$ in (16) and $\mathbf{B}_{k_g}^d$ in (17) respectively.

$$\mathbf{Q}_{k_g}^d = \sum_{\substack{j=1 \\ j \neq g}}^{G} \sum_{l=1}^{K} \sum_{m=1}^{D} P \mathbf{H}_{k_g,j} \mathbf{v}_{l_j}^m \mathbf{v}_{l_j}^{m\,H} \mathbf{H}_{k_g,j}^H + \sigma^2 \mathbf{I}_N \quad (16)$$

$$\begin{aligned}
\mathbf{B}_{k_g}^d = & \sum_{\substack{m=1 \\ m \neq d}}^{D} P \mathbf{H}_{g,k_g}^H \mathbf{u}_{k_g}^m \mathbf{u}_{k_g}^{m\,H} \mathbf{H}_{g,k_g} \\
& + \sum_{\substack{l=1 \\ l \neq k}}^{K} \sum_{m=1}^{D} P \mathbf{H}_{g,l_g}^H \mathbf{u}_{l_g}^m \mathbf{u}_{l_g}^{m\,H} \mathbf{H}_{g,l_g} \\
& + \sum_{\substack{j=1 \\ j \neq g}}^{G} \sum_{l=1}^{K} \sum_{m=1}^{D} P \mathbf{H}_{g,l_j}^H \mathbf{u}_{l_j}^m \mathbf{u}_{l_j}^{m\,H} \mathbf{H}_{g,l_j} + \sigma^2 \mathbf{I}_M \quad (17)
\end{aligned}$$

Algorithm 1 Max-SINR algorithm for the MIMO IBC

1: Initialise $\mathbf{v}_{k_g}^d$ as random unit-norm vectors, $\forall\, d, k, g$.
2: Compute the inter-cell interference plus noise covariance matrix in the forward communication channel, $\mathbf{Q}_{kg}^d$ from (16) $\forall\, d, k, g$.
3: Calculate the receive filters $\forall\, d, k, g$ using

$$\mathbf{u}_{k_g}^d = \frac{\left(\mathbf{Q}_{k_g}^d\right)^{-1} \mathbf{H}_{k_g,g} \mathbf{v}_{k_g}^d}{\left\| \left(\mathbf{Q}_{k_g}^d\right)^{-1} \mathbf{H}_{k_g,g} \mathbf{v}_{k_g}^d \right\|}.$$

4: Reverse the direction of communication and compute the total interference plus noise covariance matrix, $\mathbf{B}_{kg}^d$ from (17) $\forall\, d, k, g$.
5: Calculate the transmit beamformers $\forall\, d, k, g$ using

$$\mathbf{v}_{k_g}^d = \frac{\left(\mathbf{B}_{k_g}\right)^{-1} \mathbf{H}_{g,k_g}^H \mathbf{u}_{k_g}^d}{\left\| \left(\mathbf{B}_{k_g}\right)^{-1} \mathbf{H}_{g,k_g}^H \mathbf{u}_{k_g}^d \right\|}.$$

6: Repeat the process from step 2 until convergence or for a fixed number of iterates.

---

2) Min-WLI for the MIMO IBC: The principle behind this algorithm is to use specifically designed beamformers at each user to limit the interference experienced from all other users within the same system. The original algorithm was proposed for the IC in [22] and therefore does not cater for intra-cell interference. The key aspect in adapting it to the IBC is to treat intra-cell and inter-cell interference separately. This can be achieved by applying iterative leakage minimisation only

with respect to inter-cell leakage and then using an additional cascaded precoder to handle intra-cell interference on its own. The idea of leakage minimisation with cascaded filters has been proposed in [25] for the single-stream MIMO IBC; in this work we apply its multi-stream counterpart as outlined in Algorithm 2.

Algorithm 2 Min-WLI algorithm for the MIMO IBC

1: Initialise $\widetilde{\mathbf{V}}_g$ as a random unitary matrix $\forall\, g$.
2: Calculate the inter-cell interference covariance matrix in the forward communication channel on a per-user basis as, $\mathbf{Q}_{k_g} = \sum_{j=1, j \neq g}^{G} \mathbf{H}_{k_g,j} \widetilde{\mathbf{V}}_j \widetilde{\mathbf{V}}_j^H \mathbf{H}_{k_g,j}^H \,\forall\, k, g$.
3: The receive filter at each user is given by $\mathbf{U}_{kg} = \mathcal{V}_D[\mathbf{Q}_{k_g}]$.
4: Reverse the direction of communication and compute the inter-cell interference covariance matrix at BS g as, $\mathbf{B}_g = \sum_{j=1, j \neq g}^{G} \sum_{k=1}^{K} \mathbf{H}_{g,l_j}^H \mathbf{U}_{l_j} \mathbf{U}_{l_j}^H \mathbf{H}_{g,l_j}$ for $g = 1, \ldots, G$.
5: The first part of the transmit beamformer at BS g is given by $\widetilde{\mathbf{V}}_g = \mathcal{V}_{KD}[\mathbf{B}_g]$.
6: Repeat the process from step 2 until convergence or for a fixed number of iterates.
7: Calculate $\bar{\mathbf{V}}_g$, the additional zero-forcing precoder that handles intra-cell interference using

$$\bar{\mathbf{V}}_g = \begin{bmatrix} \mathbf{U}_{1_g}^H \mathbf{H}_{g,1_g} \widetilde{\mathbf{V}}_g \\ \vdots \\ \mathbf{U}_{K_g}^H \mathbf{H}_{g,K_g} \widetilde{\mathbf{V}}_g \end{bmatrix}^\dagger.$$

8: The overall transmit beamformer at BS g is given by, $\mathbf{V}_g = \widetilde{\mathbf{V}}_g \bar{\mathbf{V}}_g$. Taking D consecutive columns of $\mathbf{V}_g$ separately for each user k, we obtain $\mathbf{V}_{k_g}$.
9: Finally normalise $\mathbf{V}_{k_g}$ and $\mathbf{U}_{kg}$.

B. Max-SINR Algorithm With Stochastic CSI Error Knowledge (Max-SINR-SCEK)

Inspired by the CSI mismatch model used for the performance analysis, we now focus on the Max-SINR algorithm and propose a novel version that is able to handle the effect of imperfect CSI better than the standard one.

The key difference between the two algorithms is in the way the interference plus noise covariance matrices are calculated in both the forward and reverse directions when the available CSI is imperfect. For the standard Max-SINR algorithm, the imperfect CSI is used directly in place of the actual channel without any additional considerations for the effects that channel mismatch may have; thus the beamformers are calculated by replacing $\mathbf{H}$ with $\widehat{\mathbf{H}}$ directly in (16) and (17). However, in the design of the Max-SINR-SCEK algorithm we take advantage of statistical knowledge with respect to the CSI mismatch and replace the actual channel $\mathbf{H}$ with the expression in (5). This leads

to the calculation of more accurate interference plus noise co-variance matrices in both the forward and backward directions.

Therefore starting with the forward channel inter-cell interference covariance matrix in (16) and replacing $\mathbf{H}$ with (5), we get (18), given at the bottom of the page. This can be further expanded into (19), also shown at the bottom of this page. Exploiting the statistical properties of the separate components in (19) it is possible to obtain a simplified expression for the inter-cell interference plus noise covariance matrix. Since the only information available with respect to the channel uncertainty is statistical, we replace all elements of (19) containing $\mathbf{\Upsilon}$ by their expected values. Using Lemma 1 from Appendix A, $\mathbb{E}_{\mathbf{H}|\widehat{\mathbf{H}}}[\mathbf{A}] = \eta/(1+\eta)\mathbf{I}$. Also from Lemma 2, $\mathbb{E}_{\mathbf{H}|\widehat{\mathbf{H}}}[\mathbf{B}] = 0$. This allows us to obtain an improved expression for the inter-cell interference plus noise covariance matrix in the forward direction as in (20), shown at the bottom of this page, where

$$\gamma = \frac{P}{(1+\eta)^2} \tag{21}$$

and

$$\xi_f = P\frac{\eta}{(1+\eta)}(G-1)KD + \sigma^2. \tag{22}$$

Reversing the direction of communication we can calculate the interference plus noise covariance matrix for the backward channel. This is done using a method similar to the one applied in the forward communication channel to obtain (23), shown at the bottom of this page, where γ is defined as in (21) and

$$\xi_b = P\frac{\eta}{(1+\eta)}(GKD-1) + \sigma^2. \tag{24}$$

Having obtained improved expressions for the interference plus noise matrices in both directions, the novel Max-SINR-SCEK algorithm is therefore as outlined in Algorithm 3.

Algorithm 3 Max-SINR-SCEK algorithm for the MIMO IBC

1: Set γ, ξ_f and ξ_b according to (21), (22) and (24).
2: Initialise $\mathbf{v}_{k_g}^d$ as random unit-norm vectors, $\forall\, d, k, g$.
3: Calculate $\widehat{\mathbf{Q}}_{k_g}^d$ using the improved expression in (20) $\forall\, d, k, g$.
4: Obtain the receive filters $\forall\, d, k, g$ using

$$\mathbf{u}_{kg}^d = \frac{\left(\mathbf{Q}_{k_g}^d\right)^{-1}\widehat{\mathbf{H}}_{k_g,g}\mathbf{v}_{k_g}^d}{\left\|\left(\mathbf{Q}_{k_g}^d\right)^{-1}\widehat{\mathbf{H}}_{k_g,g}\mathbf{v}_{k_g}^d\right\|}.$$

5: Compute $\mathbf{B}_{k_g}^d$ using the improved expression in (23) $\forall\, d, k, g$.
6: Obtain the precoders $\forall\, d, k, g$ using

$$\mathbf{v}_{kg}^d = \frac{\left(\mathbf{B}_{k_g}^d\right)^{-1}\widehat{\mathbf{H}}_{g,k_g}^H\mathbf{u}_{k_g}^d}{\left\|\left(\mathbf{B}_{k_g}^d\right)^{-1}\widehat{\mathbf{H}}_{g,k_g}^H\mathbf{u}_{k_g}^d\right\|}.$$

7: Repeat the process from step 3 until convergence or for a fixed number of iterates.

Remark 2: We refer to γ, ξ_f and ξ_b collectively as the stochastic CSI error knowledge (SCEK) parameters, because it is the key introduction of these three elements which differenti-

---

$$\mathbf{Q}_{k_g}^d = \sum_{\substack{j=1\\j\neq g}}^{G}\sum_{l=1}^{K}\sum_{m=1}^{D} P\left(\frac{1}{1+\eta}\widehat{\mathbf{H}}_{k_g,j} + \mathbf{\Upsilon}_{k_g,j}\right)\mathbf{v}_{l_j}^m\mathbf{v}_{l_j}^{m\,H}\left(\frac{1}{1+\eta}\widehat{\mathbf{H}}_{k_g,j} + \mathbf{\Upsilon}_{k_g,j}\right)^H + \sigma^2\mathbf{I}_N \tag{18}$$

$$= \sum_{\substack{j=1\\j\neq g}}^{G}\sum_{l=1}^{K}\sum_{m=1}^{D} P\left[\frac{1}{(1+\eta)^2}\widehat{\mathbf{H}}_{k_g,j}\mathbf{v}_{l_j}^m\mathbf{v}_{l_j}^{m\,H}\widehat{\mathbf{H}}_{k_g,j}^H + \underbrace{\mathbf{\Upsilon}_{k_g,j}\mathbf{v}_{l_j}^m\mathbf{v}_{l_j}^{m\,H}\mathbf{\Upsilon}_{k_g,j}^H}_{\mathbf{A}}\right.$$

$$\left.+\frac{1}{(1+\eta)}\underbrace{\left(\widehat{\mathbf{H}}_{k_g,j}\mathbf{v}_{l_j}^m\mathbf{v}_{l_j}^{m\,H}\mathbf{\Upsilon}_{k_g,j}^H + \mathbf{\Upsilon}_{k_g,j}\mathbf{v}_{l_j}^m\mathbf{v}_{l_j}^{m\,H}\widehat{\mathbf{H}}_{k_g,j}^H\right)}_{\mathbf{B}}\right] + \sigma^2\mathbf{I}_N \tag{19}$$

$$= \sum_{\substack{j=1\\j\neq g}}^{G}\sum_{l=1}^{K}\sum_{m=1}^{D} \gamma\widehat{\mathbf{H}}_{k_g,j}\mathbf{v}_{l_j}^m\mathbf{v}_{l_j}^{m\,H}\widehat{\mathbf{H}}_{k_g,j}^H + \xi_f\mathbf{I}_N \tag{20}$$

$$\mathbf{B}_{k_g}^d = \sum_{\substack{m=1\\m\neq d}}^{D} \gamma\widehat{\mathbf{H}}_{g,k_g}^H\mathbf{u}_{k_g}^m\mathbf{u}_{k_g}^{m\,H}\widehat{\mathbf{H}}_{g,k_g} + \sum_{\substack{l=1\\l\neq k}}^{K}\sum_{m=1}^{D} \gamma\widehat{\mathbf{H}}_{g,l_g}^H\mathbf{u}_{l_g}^m\mathbf{u}_{l_g}^{m\,H}\widehat{\mathbf{H}}_{g,l_g} + \sum_{\substack{j=1\\j\neq g}}^{G}\sum_{l=1}^{K}\sum_{m=1}^{D} \gamma\widehat{\mathbf{H}}_{g,l_j}^H\mathbf{u}_{l_j}^m\mathbf{u}_{l_j}^{m\,H}\widehat{\mathbf{H}}_{g,l_j} + \xi_b\mathbf{I}_M \tag{23}$$

ates the Max-SINR-SCEK algorithm from the standard version in Algorithm 1. The advantage of the Max-SINR-SCEK algorithm is its ability to calculate improved interference covariance matrices by proper specification of these three parameters. Setting $\gamma = P$ and $\xi_f = \xi_b = \sigma^2$ in the first step of Algorithm 3 would cause it to behave exactly in the same manner as the standard version in Algorithm 1. Therefore any performance advantages obtained by the use of the novel version are obtained at no extra computational cost.

VI. SIMULATION RESULTS

This section provides simulation results to validate the analyses presented so far. It is divided into two main parts; first we confirm the validity of the bounds derived in Section IV, next in the second part we show that the Max-SINR-SCEK algorithm proposed in Section V-B does indeed provide performance improvement compared to the standard one under imperfect CSI conditions.

Throughout all our simulations the noise variance, σ^2, is fixed at 1 making the transmit signal power equivalent to the network SNR. All results presented are averaged over 250 channel realisations.

Assuming all interference is treated as noise, throughout our simulations we calculate the achievable sum rate across all users as

$$R = \sum_{g=1}^{G}\sum_{k=1}^{K} \log_2 \left| \mathbf{I}_D + \left(\sigma^2 \mathbf{I}_D + \mathbf{F}_{k_g} \right)^{-1} \mathbf{S}_{k_g} \right| \quad (25)$$

where

$$\mathbf{F}_{k_g} = \sum_{\substack{j=1 \\ (j,l) \neq (g,k)}}^{G}\sum_{l=1}^{K} P\mathbf{U}_{k_g}^H \mathbf{H}_{k_g,j}\mathbf{V}_{l_j}\mathbf{V}_{l_j}^H \mathbf{H}_{k_g,j}^H \mathbf{U}_{k_g} \quad (26)$$

$$\mathbf{S}_{k_g} = P\mathbf{U}_{k_g}^H \mathbf{H}_{k_g,g}\mathbf{V}_{k_g}\mathbf{V}_{k_g}^H \mathbf{H}_{k_g,g}^H \mathbf{U}_{k_g}. \quad (27)$$

Note that $\mathbf{F}_{k_g}$ and $\mathbf{S}_{k_g}$ are respectively the interference and the signal covariance matrices for user k in cell g. Also for imperfect CSI situations, the transmit and receive filters $\mathbf{U}$ and $\mathbf{V}$ in (26) and (27) are replaced by $\widehat{\mathbf{U}}$ and $\widehat{\mathbf{V}}$, since they are calculated based on the available imperfect CSI.

A. Simulation Results on the Theoretically Derived Bounds

In this subsection we verify the validity of the bounds derived in Theorems 1 and 2 using the two standard IA schemes outlined in Section V-A. While several MIMO IBC scenarios have been simulated, here we only present results for two specific cases.

Case 1) $G = 3$, $K = 2$, $D = 1$, $M = 4$ and $N = 4$
Case 2) $G = 2$, $K = 2$, $D = 2$, $M = 4$ and $N = 6$

In both scenarios the choice of the number of transmit and receive antennas is such that the IA feasibility conditions are met. While the two test cases were simulated with both the Max-SINR and Min-WLI algorithms, here we present only one result for each case; Fig. 2 is for Case 1 tested with the Max-
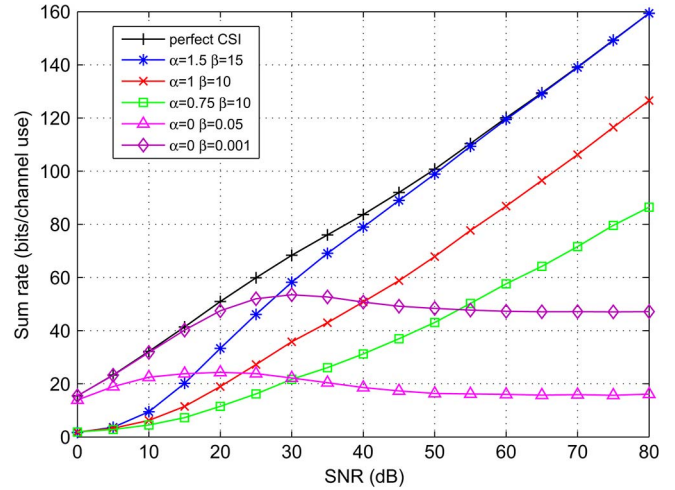

Fig. 2. Average sum rates achieved by Max-SINR algorithm under various imperfect CSI conditions for system in Case 1.
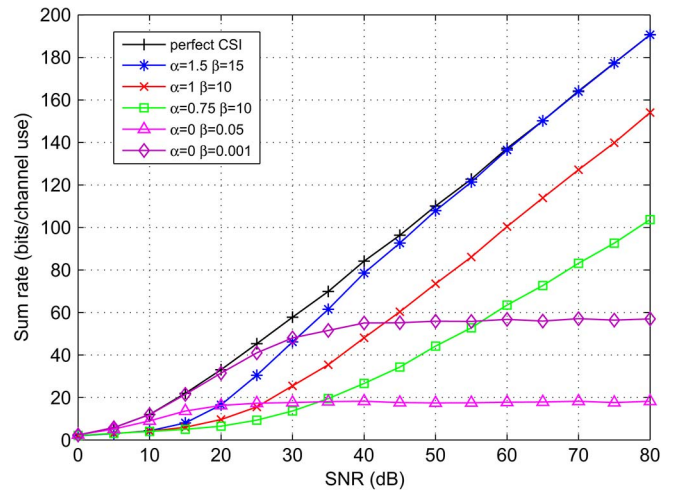

Fig. 3. Average sum rates achieved by Min-WLI algorithm under various imperfect CSI conditions for system in Case 2.

SINR algorithm, while Fig. 3 is for the Min-WLI algorithm applied to Case 2.

Note that since error variance depends on the inverse of the SNR, $\eta = \beta\rho^{-\alpha}$, to ensure that the effect of the CSI mismatch is experienced across a wide range of SNRs, then the larger the value of α, the much larger is the corresponding β value.

Considering Fig. 2, the full DoF achievable with perfect CSI is equal to $GKD = 6$. Theorem 2 predicts no DoF loss for values of $\alpha \geq 1$, which can easily be verified by focusing on the $\alpha = 1.5$ and $\alpha = 1$ results in Fig. 2. The slope for both is exactly equal to the one achieved with perfect CSI, confirming the validity of the claim in Theorem 2. One important difference between the $\alpha = 1.5$ and $\alpha = 1$ curves is the fact at high SNR the former is exactly in line with the perfect CSI result; while the latter runs parallel to it, achieving lower sum rate values overall. This behaviour is expected from the bound in Theorem 1. For $\alpha > 1$, no sum rate loss is expected at high SNR, which is exactly what happens for $\alpha = 1.5$. However, at $\alpha = 1$ the same theorem indicates that there should be a finite asymptotic sum rate loss bounded by $GKD \, \log_2(1 + \beta(GKD - 1)) \simeq 34.03$ bits per channel use for Case 1 with

$\beta = 10$. Measuring the actual loss at high SNR from Fig. 2 we obtain a value of 32.76 bits per channel use. This approaches the derived upper bound closely, verifying that it is not too loose. In addition running the same test case with the Min-WLI algorithm gave an asymptotic sum rate loss equal to 33.28 bits per channel use, showing that the bound in Theorem 1 is respected regardless of the IA technique used to test it.

When it comes to the $\alpha < 1$ range, from Theorem 1 we expect the sum rate loss to be unbounded. This can be confirmed via the $\alpha = 0.75$ and $\alpha = 0$ curves in Fig. 2. All three diverge from the perfect CSI result, indicating that the sum rate loss is growing with increasing SNR. Within the same α range, a DoF loss is expected from Theorem 2. For example at $\alpha = 0.75$, DoF equal to $\frac{3}{4}GKD = 4.5$ may be achieved, this can be easily verified from the slope of the curve itself at high SNR. The same theorem predicts zero DoF are achievable at $\alpha = 0$, which is directly reflected in the flatness of the corresponding two curves in the high SNR region of Fig. 2.

Comparing the two curves gives an insight into the impact of the β parameter; while for asymptotic analysis its effect is limited and not significant in determining the general trend of the sum rate performance, it can be noticed that at $\alpha = 0$, β has a heavier impact. In such situations the error variance η is no longer inversely proportional to SNR; thus for any fixed β, $\alpha = 0$ represents the worst case scenario, where the error variance is equal to β itself. For the two specific $\alpha = 0$ examples in Fig. 2 at $\beta = 0.05$ there is a much larger error variance than at $\beta = 0.001$. The larger the level of the CSI mismatch, the more difficult it is to achieve IA. Thus the sum rate curve for $\alpha = 0$, $\beta = 0.05$ is nearly flat throughout indicating the error is too large for IA to take place across the whole SNR range. However at $\alpha = 0$, $\beta = 0.001$ IA is achievable in the lower SNR region, up to around 20 dB, after which the saturation occurs. Since all users are allocated equal power, increasing the desired signal power inherently causes an increase in the power of the interfering signals. This makes the network interference limited, causing saturation in sum rate and leading to no advantage overall.

Fig. 3 simulates the scenario in Case 2 using the Min-WLI algorithm. Curves for $\alpha \geq 1$ all have the same slope as the perfect CSI curve, indicating that full DoF has been achieved as expected from Theorem 2. In addition, at asymptotically high SNR for the $\alpha = 1.5$ curve there is no asymptotic sum rate loss as expected from Theorem 1. For $\alpha = 1$, $\beta = 10$ the same theorem indicates that the asymptotic sum rate loss should be bounded by 49.19 bits per channel use. Measuring the actual gap from Fig. 3 a value of 37.38 bits per channel use is obtained. Additionally for the same scenario with the Max-SINR algorithm, the sum rate gap is equal to 37.61 bits per channel use. These results, combined with those obtained for the Case 1 scenario, further confirm that the bound is not excessively loose. Finally Theorem 1 states that the asymptotic sum rate loss is unbounded for the range of $\alpha < 1$; this can be confirmed from the $\alpha = 0.75$ and $\alpha = 0$ curves in Fig. 3, both of which diverge from the perfect CSI result. Within the same α range we expect the achievable DoF to be equal to αGKD. Thus at $\alpha = 0.75$ DoF equal to 6 are achievable, as verified from the slope of the curve in Fig. 3. Similarly both $\alpha = 0$
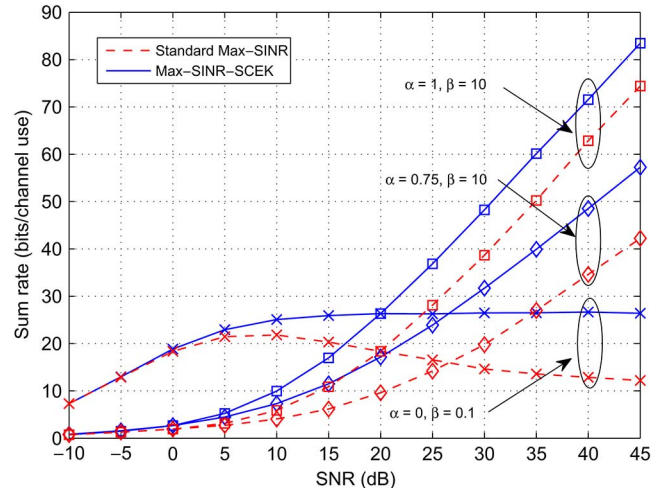

Fig. 4. Average sum rates achieved for system with $G = 3$, $K = 3$, $D = 1$ and $M = N = 5$ under various CSI imperfection scenarios.

results saturate at high SNR, denoting that $\alpha GKD = 0$ DoF are obtained i.e. IA is no longer achievable.

Remark 3: The various CSI quality scenarios simulated here can be related to the CSI acquisition techniques outlined earlier in Section II. For example, $\alpha = 0$ corresponds to the CSI feedback scenario. Looking at the corresponding results in Fig. 2 and Fig. 3 it is clear that with this CSI acquisition technique IA works better in the lower SNR region. The overall performance depends on the quality of the CSI, which for the case of $\alpha = 0$ is a function of the amount of quantisation. The lower the β, the smaller is the error due to quantisation and the better IA performs. On the other hand for reciprocal channels, modelled by $\alpha = 1$, IA fares better in the higher SNR region. In this case the CSI error is inversely proportional to SNR, therefore its effect decreases with increasing SNR, leading to a better performance by the IA techniques.

B. Simulation Results on the Performance of the Max-SINR-SCEK Algorithm

In this subsection, we compare the novel Max-SINR-SCEK algorithm proposed in Algorithm 3 to the standard one outlined in Algorithm 1. A system configuration with $G = 3$, $K = 3$, $D = 1$ and $M = N = 5$ is used to produce the sum rate and BER results in Fig. 4 and Fig. 5 respectively. We focus on the range $\alpha \leq 1$, since both Theorem 1 and Theorem 2 indicate that the system becomes asymptotically equivalent to the perfect CSI case for $\alpha > 1$.

As can be seen from Fig. 4 and Fig. 5 the Max-SINR-SCEK algorithm outperforms the standard one, both in terms of sum rate and BER. In fact the Max-SINR-SCEK algorithm achieves higher sum rates throughout, for example at $\alpha = 1$, $\beta = 10$ we obtain an 8.7 bits per channel use gain at an SNR of 40 dB, while for $\alpha = 0.75$, $\beta = 10$ the gain is equal to 13.9 bits per channel use at the same SNR. When it comes to the $\alpha = 0$, $\beta = 0.1$ case we observe that as SNR increases, the sum rate achievable by both versions of the algorithm settles at a steady value. This value is 13.8 bits per channel use higher for the Max-SINR-SCEK algorithm in comparison to the standard one. As observed earlier in Section VI-A, at $\alpha = 0$ we get the
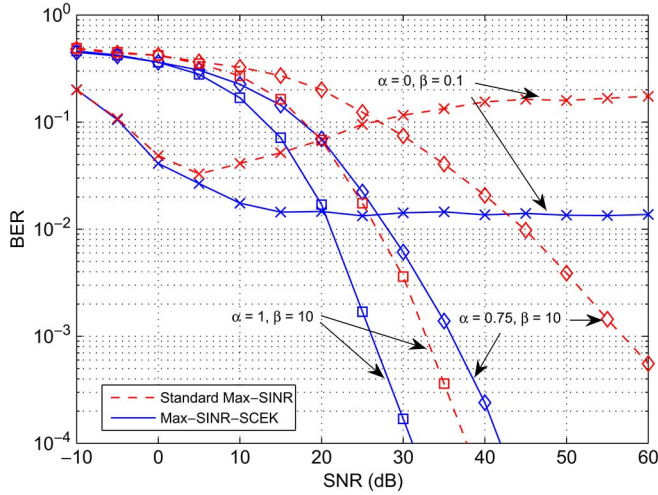
Fig. 5. BER achieved for system with $G = 3$, $K = 3$, $D = 1$ and $M = N = 5$ under various CSI imperfection scenarios.

highest level of channel uncertainty for any given β. At this level of uncertainty the network becomes interference limited and increasing transmission power provides no advantage. This effect is also mirrored into the BER results in Fig. 5, whereby the curves for $\alpha = 0$ both become flat for increasing SNR. However curves for the Max-SINR-SCEK algorithm settle at lower BER values than for the standard one, indicating the superior performance of the former.

For larger values of α, the Max-SINR-SCEK algorithm still achieves a lower BER than the standard one. For example, at $\alpha = 1$, $\beta = 10$ the standard algorithm requires an SNR of approximately 25.6 dB to achieve a BER of 10^{-2}, while Max-SINR-SCEK achieves the same BER at around 21 dB. Similarly for $\alpha = 0.75$, $\beta = 10$ Max-SINR-SCEK requires 20 dB less than standard Max-SINR to achieve a BER of 10^{-2}.

VII. CONCLUSION

IA is a very promising technique and while it has been shown that it can provide many benefits with perfect CSI, it is also important to consider the more realistic imperfect CSI scenario. In this paper we analyse the performance of IA under imperfect CSI for the MIMO IBC. A bound on the asymptotic mean loss in sum rate compared to the perfect CSI case is derived and the achievable DoF under CSI mismatch are characterised. These properties are found to be dependent on the number of cells and the amount of users per cell, in addition to the CSI mismatch parameters themselves. Results show that the way error variance scales with SNR is highly important when analysing the effects of imperfect CSI on system performance. When they are inversely proportional, full DoF can be achieved and the asymptotic sum rate loss is finite. However in cases where the error variance depends inversely on SNR to the power of a proper fraction, full DoF cannot be achieved and the asymptotic sum rate loss is unbounded. Additionally, inspired by the CSI mismatch model used, we also present a novel Max-SINR algorithm with stochastic CSI error knowledge. This algorithm performs better than the standard one under CSI mismatch and at no additional computational cost.

APPENDIX A
USEFUL LEMMAS

Lemma 1: If $\mathbf{F} \in \mathbb{C}^{M \times N}$ is a Gaussian matrix whose elements are i.i.d. with zero mean and variance ν, and $\mathbf{g} \in \mathbb{C}^{N \times 1}$ is a unit-norm vector that is independent of $\mathbf{F}$, then $\mathbb{E}_{\mathbf{F}}[\mathbf{F}\mathbf{g}\mathbf{g}^H\mathbf{F}^H] = \nu I$.

Proof: Consider a unitary matrix $\mathbf{G} \in \mathbb{C}^{N \times N}$ that is independent of $\mathbf{F}$. Since $\mathbf{F}$ is a Gaussian matrix, it is bi-unitarily invariant [31], hence the joint distribution of the product $\mathbf{FG}$ is equal to that of $\mathbf{F}$ itself. Additionally, since matrix $\mathbf{G}$ consists of N unit-norm vectors of size $N \times 1$, the vector $\mathbf{g}$ described in the definition of Lemma 1 above can take the role of any column vector within $\mathbf{G}$ itself. Thus, vector $\mathbf{Fg}$ can be considered to be a column vector of matrix $\mathbf{FG}$, which finally allows to establish the fact that $\mathbf{Fg}$ is a Gaussian vector with zero mean and covariance matrix νI. ∎

Lemma 2: $\mathbb{E}_{\mathbf{H}|\widehat{\mathbf{H}}}[\widehat{\mathbf{H}}_{k_g,j}\mathbf{v}_{l_j}^m \mathbf{v}_{l_j}^{m\,H}\boldsymbol{\Upsilon}_{k_g,j}^H] = \mathbb{E}_{\mathbf{H}|\widehat{\mathbf{H}}}[\boldsymbol{\Upsilon}_{k_g,j}\mathbf{v}_{l_j}^m \mathbf{v}_{l_j}^{m\,H}\widehat{\mathbf{H}}_{k_g,j}^H] = 0 \; \forall \, m, l, j.$

Proof: Beamforming elements are calculated using $\widehat{\mathbf{H}}_{k_g,j}$, thus they are automatically independent of $\boldsymbol{\Upsilon}_{k_g,j}$ from the definition of the imperfect CSI model in Section II. ∎

Lemma 3: $\mathbb{E}[|\widehat{\boldsymbol{u}}_{k_g}^{d\,H}\boldsymbol{\Upsilon}_{k_g,j}\widehat{\boldsymbol{v}}_{l_j}^m|^2]$ is equal to $\eta/(1+\eta)$.

Proof: From the error model definition in Section II we know that $\widehat{\mathbf{H}}_{k_g,j}$ and $\boldsymbol{\Upsilon}_{k_g,j}$ are independent. Since $\widehat{\boldsymbol{u}}_{k_g}^d$ and $\widehat{\boldsymbol{v}}_{l_j}^m$ are calculated on $\widehat{\mathbf{H}}_{k_g,j}$, this makes the transmit and receive beamformers automatically independent of $\boldsymbol{\Upsilon}_{k_g,j}$. In addition $\boldsymbol{\Upsilon}_{k_g,j}$ is Gaussian and bi-unitarily invariant [31], thereby the product $\widehat{\boldsymbol{u}}_{k_g}^{d\,H}\boldsymbol{\Upsilon}_{k_g,j}\widehat{\boldsymbol{v}}_{l_j}^m \; \forall \, d, k, g, m, l, j$ is a Gaussian random variable with zero mean and variance $\eta/(1+\eta)$. Finally using central absolute moments, we can evaluate $\mathbb{E}[|\widehat{\boldsymbol{u}}_{k_g}^{d\,H}\boldsymbol{\Upsilon}_{k_g,j}\widehat{\boldsymbol{v}}_{l_j}^m|^2]$ which is equal to $\eta/(1+\eta)$. ∎

APPENDIX B
PROOF OF THEOREM 1

Sum rate loss is defined as the difference between the sum rate achievable with perfect CSI and the sum rate achievable with imperfect CSI, taking expectations this is equivalent to

$$\Delta R = \mathbb{E}_{\mathbf{H}}\left[\sum_{g=1}^{G}\sum_{k=1}^{K}\sum_{d=1}^{D}\log_2\left(1 + \frac{P\left|\mathbf{u}_{k_g}^{dH}\mathbf{H}_{k_g,g}\mathbf{v}_{k_g}^d\right|^2}{\sigma^2}\right)\right]$$
$$-\mathbb{E}_{\mathbf{H}|\widehat{\mathbf{H}}}\left[\sum_{g=1}^{G}\sum_{k=1}^{K}\sum_{d=1}^{D}\log_2\left(1 + \frac{P\left|\widehat{\mathbf{u}}_{k_g}^{dH}\mathbf{H}_{k_g,g}\widehat{\mathbf{v}}_{k_g}^d\right|^2}{\widehat{J}_{k_g}^d + \sigma^2}\right)\right] \quad (28)$$

where $\mathbf{u}_{k_g}^d$ and $\mathbf{v}_{k_g}^d$ are single column elements of $\mathbf{U}_{k_g}$ and $\mathbf{V}_{k_g}$ obtained using perfect CSI, $\widehat{\mathbf{u}}_{k_g}^d$ and $\widehat{\mathbf{v}}_{k_g}^d$ are their imperfect CSI equivalents and $\widehat{J}_{k_g}^d$ represents the leaked interference due to imperfect CSI. After some algebraic manipulations (28) can be expressed as in (29) on the following page.

$$\Delta R = \mathbb{E}_{\mathbf{H}} \underbrace{\left[\sum_{g=1}^{G} \sum_{k=1}^{K} \sum_{d=1}^{D} \log_2 \left(1 + \frac{P \left| \mathbf{u}_{k_g}^{dH} \mathbf{H}_{k_g,g} \mathbf{v}_{k_g}^{d} \right|^2}{\sigma^2} \right) \right]}_{\mathbf{A}}$$

$$- \mathbb{E}_{\mathbf{H}|\widehat{\mathbf{H}}} \underbrace{\left[\sum_{g=1}^{G} \sum_{k=1}^{K} \sum_{d=1}^{D} \log_2 \left(1 + \frac{\widehat{J}_{k_g}^{d} + P \left| \widehat{\mathbf{u}}_{k_g}^{dH} \mathbf{H}_{k_g,g} \widehat{\mathbf{v}}_{k_g}^{d} \right|^2}{\sigma^2} \right) \right]}_{\mathbf{B}}$$

$$+ \mathbb{E}_{\mathbf{H}|\widehat{\mathbf{H}}} \left[\sum_{g=1}^{G} \sum_{k=1}^{K} \sum_{d=1}^{D} \log_2 \left(1 + \frac{\widehat{J}_{k_g}^{d}}{\sigma^2} \right) \right] \qquad (29)$$

Considering parts A and B from (29) separately we can establish an upper bound on each by applying Jensen's inequality. It can easily be shown that $|\mathbf{u}_{k_g}^{d\,H} \mathbf{H}_{k_g,g} \mathbf{v}_{k_g}^{d}|^2$ and $|\widehat{\mathbf{u}}_{k_g}^{d\,H} \mathbf{H}_{k_g,g} \widehat{\mathbf{v}}_{k_g}^{d}|^2$ are exponentially distributed with zero mean and variance one. Applying this information into the upper bounds for A and B, allows us to express the following inequality.

$$\mathbb{E}_{\mathbf{H}} \left[\sum_{g=1}^{G} \sum_{k=1}^{K} \sum_{d=1}^{D} \log_2 \left(1 + \frac{P \left| \mathbf{u}_{k_g}^{dH} \mathbf{H}_{k_g,g} \mathbf{v}_{k_g}^{d} \right|^2}{\sigma^2} \right) \right]$$

$$\leq \mathbb{E}_{\mathbf{H}|\widehat{\mathbf{H}}} \left[\sum_{g=1}^{G} \sum_{k=1}^{K} \sum_{d=1}^{D} \log_2 \left(1 + \frac{\widehat{J}_{k_g}^{d} + P \left| \widehat{\mathbf{u}}_{k_g}^{dH} \mathbf{H}_{k_g,g} \widehat{\mathbf{v}}_{k_g}^{d} \right|^2}{\sigma^2} \right) \right]$$

$$(30)$$

Next, taking into account the inequality in (30), we can express (29) as

$$\Delta R \leq \mathbb{E}_{\mathbf{H}|\widehat{\mathbf{H}}} \left[\sum_{g=1}^{G} \sum_{k=1}^{K} \sum_{d=1}^{D} \log_2 \left(1 + \frac{\widehat{J}_{k_g}^{d}}{\sigma^2} \right) \right]. \qquad (31)$$

This can be turned into the following expression by taking only the expectation of the interference leakage term according to Jensen's inequality,

$$\Delta R \leq \sum_{g=1}^{G} \sum_{k=1}^{K} \sum_{d=1}^{D} \log_2 \left(1 + \frac{\mathbb{E}_{\mathbf{H}|\widehat{\mathbf{H}}} \left[\widehat{J}_{k_g}^{d} \right]}{\sigma^2} \right). \qquad (32)$$

Therefore to quantify ΔR it is necessary to find an expression for $\mathbb{E}_{\mathbf{H}|\widehat{\mathbf{H}}}[\widehat{J}_{k_g}^{d}]$. $\widehat{J}_{k_g}^{d}$ itself has been previously defined in (12). Combining this expression with the channel model from (5) and then taking expectations we obtain

$$\sum_{\substack{m=1 \\ m \neq d}}^{D} P \mathbb{E}_{\widehat{\mathbf{H}}, \boldsymbol{\Upsilon}} \left[\left| \widehat{\mathbf{u}}_{k_g}^{dH} \left(\frac{1}{1+\eta} \widehat{\mathbf{H}}_{k_g,g} + \boldsymbol{\Upsilon}_{k_g,g} \right) \widehat{\mathbf{v}}_{k_g}^{m} \right|^2 \right]$$

$$+ \sum_{\substack{l=1 \\ l \neq k}}^{K} \sum_{m=1}^{D} P \mathbb{E}_{\widehat{\mathbf{H}}, \boldsymbol{\Upsilon}} \left[\left| \widehat{\mathbf{u}}_{k_g}^{dH} \left(\frac{1}{1+\eta} \widehat{\mathbf{H}}_{k_g,g} + \boldsymbol{\Upsilon}_{k_g,g} \right) \widehat{\mathbf{v}}_{l_g}^{m} \right|^2 \right]$$

$$+ \sum_{\substack{j=1 \\ j \neq g}}^{G} \sum_{l=1}^{K} \sum_{m=1}^{D} P \mathbb{E}_{\widehat{\mathbf{H}}, \boldsymbol{\Upsilon}} \left[\left| \widehat{\mathbf{u}}_{k_g}^{dH} \left(\frac{1}{1+\eta} \widehat{\mathbf{H}}_{k_g,j} + \boldsymbol{\Upsilon}_{k_g,j} \right) \widehat{\mathbf{v}}_{l_j}^{m} \right|^2 \right]$$

$$(33)$$

which can be further simplified by considering the IA conditions for imperfect CSI in (11). Applying the fact that $\widehat{\mathbf{u}}_{k_g}^{d\,H} \widehat{\mathbf{H}}_{k_g,j} \widehat{\mathbf{v}}_{jl}^{m} = 0 \ \forall \ (d,k,g) \neq (m,l,j)$ leads to

$$\mathbb{E}_{\mathbf{H}|\widehat{\mathbf{H}}} \left[\widehat{J}_{k_g}^{d} \right] = \sum_{\substack{m=1 \\ m \neq d}}^{D} P \mathbb{E}_{\widehat{\mathbf{H}}, \boldsymbol{\Upsilon}} \left[\left| \widehat{\mathbf{u}}_{k_g}^{dH} \boldsymbol{\Upsilon}_{k_g,g} \widehat{\mathbf{v}}_{k_g}^{m} \right|^2 \right]$$

$$+ \sum_{\substack{l=1 \\ l \neq k}}^{K} \sum_{m=1}^{D} P \mathbb{E}_{\widehat{\mathbf{H}}, \boldsymbol{\Upsilon}} \left[\left| \widehat{\mathbf{u}}_{k_g}^{dH} \boldsymbol{\Upsilon}_{k_g,g} \widehat{\mathbf{v}}_{l_g}^{m} \right|^2 \right]$$

$$+ \sum_{\substack{j=1 \\ j \neq g}}^{G} \sum_{l=1}^{K} \sum_{m=1}^{D} P \mathbb{E}_{\widehat{\mathbf{H}}, \boldsymbol{\Upsilon}} \left[\left| \widehat{\mathbf{u}}_{k_g}^{dH} \boldsymbol{\Upsilon}_{k_g,j} \widehat{\mathbf{v}}_{l_j}^{m} \right|^2 \right].$$

$$(34)$$

Integrating the result of Lemma 3 from Appendix A into (34), then the expected value for the interference leakage can be expressed as

$$\mathbb{E}_{\mathbf{H}|\widehat{\mathbf{H}}} \left[\widehat{J}_{k_g}^{d} \right] = P \frac{\eta}{(\eta + 1)} (GKD - 1). \qquad (35)$$

This can be applied into the inequality for sum rate loss from (32) to get

$$\Delta R \leq \sum_{g=1}^{G} \sum_{k=1}^{K} \sum_{d=1}^{D} \log_2 \left(1 + \frac{P}{\sigma^2} \frac{\eta}{(\eta + 1)} (GKD - 1) \right) \quad (36)$$

which after evaluating the summation and replacing η with $\beta \rho^{-\alpha}$, becomes

$$\Delta R \leq GKD \log_2 \left(1 + (GKD - 1) \frac{\beta \rho^{(1-\alpha)}}{1 + \beta \rho^{-\alpha}} \right). \qquad (37)$$

Taking a high SNR approximation, the asymptotic sum rate loss can be defined as in (14), proving Theorem 1 as originally stated.

APPENDIX C
PROOF OF THEOREM 2

The DoF loss is defined as $\Delta DoF = DoF_{\text{perfect CSI}} - DoF_{\text{imperfect CSI}}$. From (10) we have already established that the DoF achievable under perfect CSI is equal to GKD. Thus we only need to evaluate the total achievable DoF under imperfect CSI, $DoF_{\text{imperfect CSI}}$. Provided IA feasibility conditions are met, this can represented as

$$DoF_{\text{imperfect CSI}} = \lim_{P \to \infty} \frac{\mathbb{E}_{\mathbf{H}|\widehat{\mathbf{H}}} [R_{\text{imperfect CSI}}]}{\log_2 P} \qquad (38)$$

where $R_{\text{imperfect CSI}}$ was defined earlier in (13).

$$DoF_{\text{imperfect CSI}} = \lim_{P \to \infty} \underbrace{\frac{\mathbb{E}_{\mathbf{H}|\widehat{\mathbf{H}}}\left[\sum_{g=1}^{G}\sum_{k=1}^{K}\sum_{d=1}^{D}\log_2\left(P\left|\widehat{\mathbf{u}}_{k_g}^{dH}\mathbf{H}_{k_g,g}\widehat{\mathbf{v}}_{k_g}^{d}\right|^2 + \widehat{J}_{k_g}^{d} + \sigma^2\right)\right]}{\log_2 P}}_{\mathbf{A}}$$

$$-\lim_{P \to \infty}\underbrace{\frac{\mathbb{E}_{\mathbf{H}|\widehat{\mathbf{H}}}\left[\sum_{g=1}^{G}\sum_{k=1}^{K}\sum_{d=1}^{D}\log_2\left(\widehat{J}_{k_g}^{d} + \sigma^2\right)\right]}{\log_2 P}}_{\mathbf{B}} \tag{39}$$

$$\geq \lim_{P \to \infty}\frac{\mathbb{E}_{\mathbf{H}|\widehat{\mathbf{H}}}\left[\sum_{g=1}^{G}\sum_{k=1}^{K}\sum_{d=1}^{D}\log_2\left(P|\widehat{\mathbf{u}}_{k_g}^{dH}\mathbf{H}_{k_g,g}\widehat{\mathbf{v}}_{k_g}^{d}|^2\right)\right]}{\log_2 P} - \lim_{P \to \infty}\frac{\sum_{g=1}^{G}\sum_{k=1}^{K}\sum_{d=1}^{D}\log_2\left(\mathbb{E}_{\mathbf{H}|\widehat{\mathbf{H}}}\left[\widehat{J}_{k_g}^{d}\right] + \sigma^2\right)}{\log_2 P} \tag{40}$$

$$= GKD - \lim_{P \to \infty}\frac{\sum_{g=1}^{G}\sum_{k=1}^{K}\sum_{d=1}^{D}\log_2\left(P^{\frac{\eta}{(\eta+1)}}(GKD-1) + \sigma^2\right)}{\log_2 P} \tag{41}$$

Including the imperfect CSI sum rate expression from (13) into (38) and performing some additional algebraic manipulations we obtain (39), shown at the top of this page. The inequality in (40) follows by discarding the interference plus noise term in part A and applying Jensen's inequality to part B.

Finally the DoF expression can be transformed into (41), shown at the top of this page, by using the fact that $|\widehat{\boldsymbol{u}}_{k_g}^{d\,H}\mathbf{H}_{k_g,g}\widehat{\boldsymbol{v}}_{k_g}^{d}|^2$ is exponentially distributed with zero mean and variance one and also replacing $\mathbb{E}_{\mathbf{H}|\widehat{\mathbf{H}}}[\widehat{J}_{k_g}^{d}]$ by the actual expression from (35).

After replacing η with $\beta P^{-\alpha}\sigma^{2\alpha}$ in (41) and taking $P \to \infty$, the achievable DoF can be characterised as

$$DoF_{\text{imperfect CSI}} = \begin{cases} GKD & \alpha \geq 1 \\ \alpha GKD & 0 \leq \alpha < 1. \end{cases} \tag{42}$$

Noting that $DoF_{\text{perfect CSI}} = GKD$ from (10), the result in (15) is obtained, proving the DoF loss is as originally stated in Theorem 2.

REFERENCES

[1] S. A. Jafar, "Interference alignment: A new look at signal dimensions in a communication network," *Found. Trends Commun. Inf. Theory*, vol. 7, no. 1, pp. 1–136, Jun. 2011.

[2] V. R. Cadambe and S. A. Jafar, "Interference alignment and degrees of freedom of the K-user interference channel," *IEEE Trans. Inf. Theory*, vol. 54, no. 8, pp. 3425–3441, Aug. 2008.

[3] O. El Ayach, A. Lozano, and R. W. Heath, "On the overhead of interference alignment: Training, feedback, and cooperation," *IEEE Trans. Wireless Commun.*, vol. 11, no. 11, pp. 4192–4203, Nov. 2012.

[4] H. Bolcskei and I. J. Thukral, "Interference alignment with limited feedback," in *Proc. IEEE ISIT*, Jul. 2009, pp. 1759–1763.

[5] R. T. Krishnamachari and M. K. Varanasi, "Interference alignment under limited feedback for MIMO interference channels," *IEEE Trans. Signal Process.*, vol. 61, no. 15, pp. 3908–3917, Aug. 2013.

[6] B. Nosrat-Makouei, J. G. Andrews, and R. W. Heath, "MIMO interference alignment over correlated channels with imperfect CSI," *IEEE Trans. Signal Process.*, vol. 59, no. 6, pp. 2783–2794, Jun. 2011.

[7] O. E. Ayach and R. W. Heath, "Interference alignment with analog channel state feedback," *IEEE Trans. Wireless Commun.*, vol. 11, no. 2, pp. 626–636, Feb. 2012.

[8] R. Tresch and M. Guillaud, "Cellular interference alignment with imperfect channel knowledge," in *Proc. IEEE Int. Conf. Commun.*, Jun. 2009, pp. 1–5.

[9] C. Suh and D. Tse, "Interference alignment for cellular networks," in *Proc. 46th Annu. Allerton Conf. Commun., Control, Comput.*, Sep. 2008, pp. 1037–1044.

[10] J. Kim, S. H. Park, H. Sung, and I. Lee, "Spatial multiplexing gain for two interfering MIMO broadcast channels based on linear transceiver," *IEEE Trans. Wireless Commun.*, vol. 9, no. 10, pp. 3012–3017, Oct. 2010.

[11] G. Sridharan and W. Yu, "Degrees of freedom of MIMO cellular networks with two cells and two users per cell," in *Proc. IEEE ISIT*, Jul. 2013, pp. 1774–1778.

[12] S. H. Park and I. Lee, "Degrees of freedom of multiple broadcast channels in the presence of inter-cell interference," *IEEE Trans. Commun.*, vol. 59, no. 5, pp. 1481–1487, May 2011.

[13] T. Kim, D. J. Love, B. Clerckx, and D. Hwang, "Spatial degrees of freedom of the multicell mimo multiple access channel," in *Proc. IEEE GLOBECOM*, Dec. 2011, pp. 1–5.

[14] T. Liu and C. Yang, "Degrees of freedom of general symmetric MIMO interference broadcast channels," in *Proc. IEEE ICASSP*, May 2013, pp. 4364–4368.

[15] G. Sridharan and W. Yu, "Degrees of freedom of MIMO cellular networks: Decomposition and linear beamforming design," 2013. [Online]. Available: http://arxiv.org/abs/1312.2681

[16] T. Liu and C. Yang, "On the degrees of freedom of asymmetric MIMO interference broadcast channels," in *Proc. IEEE ICC*, Jun. 2014, pp. 1971–1976.

[17] T. Liu and C. Yang, "On the feasibility of linear interference alignment for MIMO interference broadcast channels with constant coefficients," *IEEE Trans. Signal Process.*, vol. 61, no. 9, pp. 2178–2191, May 2013.

[18] Y. Ma, J. Li, R. Chen, and Q. Liu, "On feasibility of interference alignment for L-cell constant cellular interfering networks," *IEEE Commun. Lett.*, vol. 16, no. 5, pp. 714–716, May 2012.

[19] M. Guillaud and D. Gesbert, "Interference alignment in partially connected interfering multiple-access and broadcast channels," in *Proc. IEEE GLOBECOM*, Dec. 2011, pp. 1–5.

[20] S. Razavi and T. Ratnarajah, "Performance analysis of interference alignment under CSI mismatch," *IEEE Trans. Veh. Technol.*, vol. 63, no. 9, pp. 4740–4748, Nov. 2014.

[21] J. Maurer, J. Jaldén, D. Seethaler, and G. Matz, "Vector perturbation precoding revisited," *IEEE Trans. Signal Process.*, vol. 59, no. 1, pp. 315–328, Jan. 2011.

[22] K. Gomadam, V. R. Cadambe, and S. A. Jafar, "A distributed numerical approach to interference alignment and applications to wireless interference networks," *IEEE Trans. Inf. Theory*, vol. 57, no. 6, pp. 3309–3322, Jun. 2011.

[23] B. Zhuang, R. A. Berry, and M. L. Honig, "Interference alignment in MIMO cellular networks," in *Proc. IEEE ICASSP*, May 2011, pp. 3356–3359.

[24] J. Schreck and G. Wunder, "Distributed interference alignment in cellular systems: Analysis and algorithms," in *Proc. 11th Eur. Wireless Conf.—Sustainable Wireless Technol.*, Apr. 2011, pp. 1–8.

[25] R. K. Mungara, A. Tolli, and M. Juntti, "Degrees of freedom and interference mitigation for MIMO interfering broadcast channels," in *Proc. IEEE GLOBECOM*, Dec. 2011, pp. 441–446.

[26] J. Park, Y. Sung, and H. V. Poor, "On beamformer design for multiuser MIMO interference channels," 2010. [Online]. Available: http://arxiv.org/abs/1011.6121

[27] I. Santamaria, O. Gonzalez, R. W. Heath, and S. W. Peters, "Maximum sum-rate interference alignment algorithms for MIMO channels," in *Proc. IEEE GLOBECOM*, Dec. 2010, pp. 1–6.

[28] C. Wilson and V. V. Veeravalli, "A convergent version of the Max SINR algorithm for the MIMO interference channel," *IEEE Trans. Wireless Commun.*, vol. 12, no. 6, pp. 2952–2961, Jun. 2013.

[29] T. Yoo and A. Goldsmith, "Capacity and power allocation for fading MIMO channels with channel estimation error," *IEEE Trans. Inf. Theory*, vol. 52, no. 5, pp. 2203–2214, May 2006.

[30] S. M. Kay, *Fundamentals of Statistical Signal Processing: Estimation Theory*. Englewood Cliffs, NJ, USA: Prentice-Hall, 1993.

[31] A. M. Tulino and S. Verdu, "Random matrix theory and wireless communications," *Found. Trends Commun. Inf. Theory*, vol. 1, no. 1, pp. 1–182, Jun. 2004.

Paula Aquilina (S'14) received the B.Eng. (Hons.) degree in electrical engineering from the University of Malta in 2010 and the M.Sc. degree in signal processing and communications from the University of Edinburgh in 2013. She is currently pursuing the Ph.D. degree at the University of Edinburgh's Institute for Digital Communications. Her research interests include various topics in wireless communications and network information theory with particular focus on interference management.

Tharmalingam Ratnarajah (A'96–M'05–SM'05) is currently with the Institute for Digital Communications, University of Edinburgh, Edinburgh, U.K., as a Reader in signal processing and communications. His research interests include random matrices theory, information theoretic and signal processing aspects of 5G wireless networks, statistical and array signal processing, biomedical signal processing, and quantum information theory. He has published over 250 publications in these areas and holds four U.S. patents. He is currently the coordinator of the FP7 projects HARP (3.2M€) in the area of highly distributed MIMO and ADEL (3.7M€) in the area of dynamic spectrum access. Previously, he was the coordinator of FP7 Future and Emerging Technologies project CROWN (2.3Meuros) in the area of cognitive radio networks and HIATUS (2.7M€) in the area of interference alignment. Dr. Ratnarajah is a member of the American Mathematical Society and Information Theory Society and Fellow of Higher Education Academy (FHEA), U.K.